Molecular Simulation Study of Polymer Interactions with Silica Particles in Aqueous Solution

Han C. Lay,[†] Michelle J. S. Spencer,[†] Evan J. Evans,[‡] and Irene Yarovsky*,[†]

Department of Applied Physics, RMIT University GPO Box 2476V, Melbourne VIC 3001, Australia, and BHP Steel Research Laboratories, Port Kembla, Australia

This paper describes computational modeling of interactions between components of organic/inorganic polymer hybrid (OIPH) materials, particularly polymer interactions with colloidal silica particles in aqueous solution. Particle surface models have been developed and molecular dynamics simulations applied to a range of systems representing various separations between the particles and different polymer solution concentrations. The equilibrium structures and specific interactions between the polymer, solvent, and silica surfaces with different surface modifications have been examined and molecular mechanisms of interactions involved in the formation of the nanocomposite materials have been suggested. The results presented in this paper complement our previous study of the interactions between precursors used in the synthesis of the OIPHs, thus providing a more complete picture of the atomistic details and mechanisms of interactions between the components of the OIPH materials at various stages of their formation.

1. Background

Organic/inorganic polymer hybrid (OIPH) materials are currently attracting a lot of interest from industry and academia because of their unique properties and the relative ease to manipulate them via targeted selection of precursors and synthetic routes. OIPHs are nanocomposite materials constructed at the atomic level. In most cases, the constituents are mixed or synthesized to form physical hybrids. These hybrids display strong interactions at interfaces even though they are not true copolymers. Common systems include silica, titania, alumina, and zirconia as the nanoparticles cross-linked or polymerized to form a hybrid network. Typical steps in their formation may involve the mixture of inorganic precursors and polymer constituents (and also stoichiometric amounts of water) to form the sol–solid suspended in liquid. The gel–liquid suspended in solid, is formed from the controlled hydrolysis and condensation of the inorganic precursors with each other and/or with the polymer constituents to create the hybrid network.

One of the properties of OIPH materials—increased hardness while retaining flexibility—makes them valuable in a wide range of applications, particularly in coatings.[1,2] This property is due to complementary contributions from the inorganic component (silica), which adds hardness to the resultant product, and from the polymeric component, which adds flexibility.[3–7] Several hypotheses have been suggested to explain the molecular mechanisms of formation of the hybrid materials, based primarily on experimental measurements during various stages of the sol–gel process, the common method for preparation of inorganic amorphous solids.[3,4]

Investigations of the synthesis of aqueous sol–gel systems include the work by Schmidt et al.,[1] which involved the preparation of coating precursors that are soluble in water, by modifying commercially available sols with alkoxysilanes (reducing the particle to particle interaction), to fabricate an aqueous sol–gel coating material. It was found that the water stability of these coating materials is comparable to the alcohol-based systems and the process can be used to incorporate other nanoparticles such as titania or alumina.

Hoffmann and Amberg-Schwab[2] investigated the oxygen barrier properties of organic–inorganic polymers by analyzing the oxygen transmission rate with respect to organic and inorganic network densities of the final materials. It was found that by increasing the inorganic (raising the tetramethoxysilane (TMOS) content in the sol) or the organic network density (extending the curing time), the oxygen transmission rate was reduced.

Kumudine and Mark[7] used in situ precipitation techniques to reinforce poly(dimethylsiloxane) (PDMS). The technique involved the introduction of silica filler particles within the polymer network produced from catalytic hydrolysis of tetra-ethoxysilane (TEOS). Portions of the PDMS were mixed with TEOS, and the hydrolysis and condensation of TEOS present in excess of the stoichiometric balance produced silica within the network. It was found that the degradation temperature of the material increased with the amount of filler incorporated. It was also found that the tear strength of the material was increased with the presence of the filler particle, causing uneven tear paths.

A further example of investigations into synthesis of physical hybrids include the work performed by Klein et al.[3] which examined the mechanical properties of hybrids created via the sol–gel method. Samples containing poly(ethyleneoxide) (PEO) or poly(vinyl acetate) (PVAc) were prepared by mixing tetra-ethyl orthosilicate with water or a water/ethanol mixture. It was found that interactions between the polymer and the silica network occurred largely via hydrogen bonding between oxygens and silanols in the PEO samples, and hydroxyls and silanols

---

[†] RMIT University.
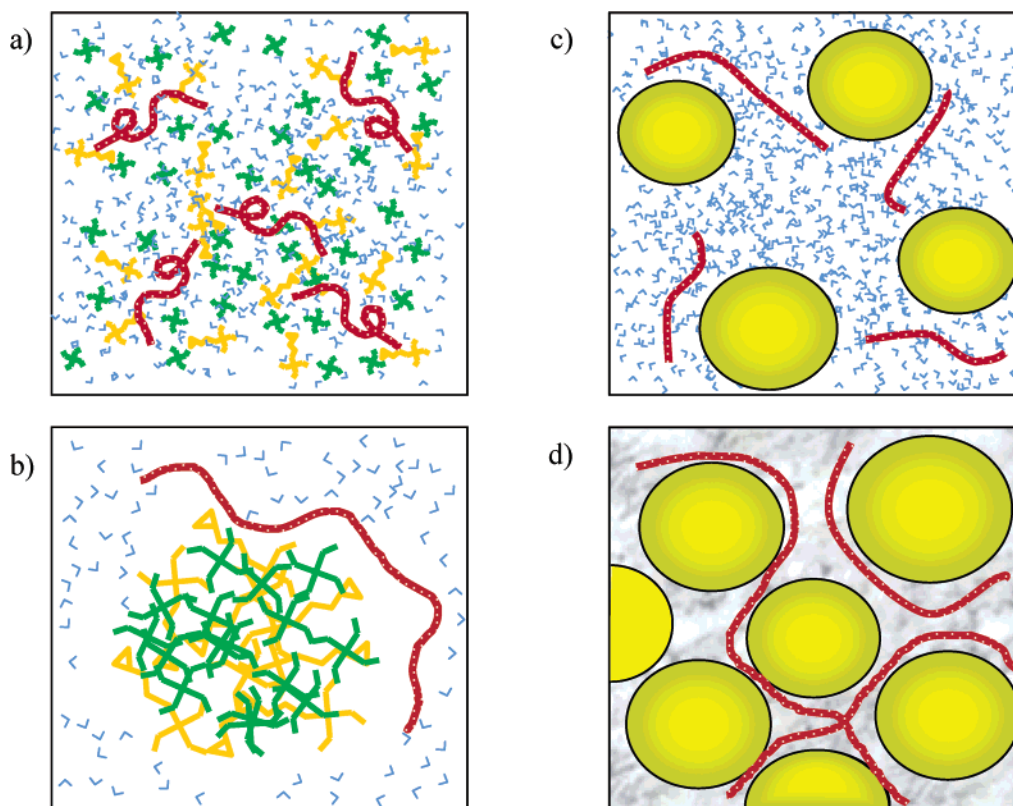[‡] BHP Steel Research Laboratories.

Figure 1. Formation of OIPH materials. (a) Initial aqueous solution of precursors and polymer molecules. (b) Aggregates form by self-association of precursors due to the hydrophobic effect; precursors hydrolyze; polymer molecule attaches to the aggregate. (c) SiO₂ bonds form within the aggregates, producing silica particles. Alcohol residues are eliminated during formation of the particle, with some residual groups staying chemically bonded to the particle surface (not shown). (d) System is dried to form a solid-state OIPH material.

in the PVAc samples. It was also found that the extent of this bonding increased with aging time.

The above examples, chosen from a very extensive body of recent literature on hybrid materials, demonstrate that it is necessary to develop a molecular level understanding of the formation mechanisms of the materials because, through the choice of precursors, reaction and drying conditions, materials with desired properties may be designed.

Theoretical molecular modeling is now widely recognized for producing useful insights into molecular interactions in materials that can complement experimental data and, in some cases, provide fundamental information that is difficult or impossible to obtain experimentally. For example, molecular dynamics (MD) simulations have been demonstrated to provide structural and dynamic information on aqueous systems, including polymer hydrogels, that is unavailable by any other method.[8,9] A good example of MD simulations of polymer hydrogels is the study of hydrogen bond structure and dynamics of poly(vinyl alcohol) (PVA), poly(vinyl methyl ether) (PVME), and poly(*N*-isopropylacrylamide) (PNiPAM) in water by Tamai et al.[10] Using the definition of hydrogen bonds adopted from Luzar and Chandler,[11] they classified water molecules in the polymer hydrogel systems into three categories (hydrophilic, hydrophobic, and bulk), and evaluated the structural and dynamic properties of hydrogen bonds in these regions. It was found that the water–water hydrogen bonds were enhanced around hydrophobic groups and that the mobility of water molecules around the polymer chain was lowered significantly.

MD has also become a promising tool for the calculation of diffusion coefficients and solubility parameters of polymers and small molecules. Nick and Suter[12] demonstrated the application of MD to study the solubility of water in polymers and to determine the equilibrium water content using a two-step method that combines a thermodynamic integration approach and Widom's particle insertion method.[13]

Muller-Plathe et al.[14] also made extensive studies on the solvation of PVA in three different solutions (water, ethanol, and a 1/1 mixture) using MD. It was discovered, through radial distribution function (RDF) and mean square displacement (MSD) analysis, that water–water hydrogen bonding was slightly shorter lived than polymer–water hydrogen bonds. Furthermore, it was found that the small size of the water molecules allowed the OH groups of the PVA to simultaneously form more hydrogen bonds to water (as compared to ethanol) due to geometric reasons.

Further relevant examples of MD simulations include the study by Gestoso and Brisson of the effects of hydrogen bonds in poly(vinyl phenol) (PVPh).[15] They demonstrated that molecular simulations allow the calculation of intrachain hydrogen bonds which cannot be determined experimentally. It was also shown that the hydrogen bonds in PVPh rigidify the polymer and increase both inter- and intrachain interaction. Furthermore, these reactions were related to the decrease in the radius of gyration and the increase in the glass transition temperature.

MD simulations have been previously employed to better understand the molecular interactions at the initial stages of the sol–gel process in preparation of select OIPH materials.[16,17] These studies involved the construction of molecular models of aqueous solutions, which contained organofunctionalized silanes ([(glycidyloxy)propyl]trimethoxysilane (ES), tetraethoxysilane (TEOS)) and the polymer constituent poly(vinyl alcohol) (PVA), to represent various model stages of the hydrolysis reaction. Information about the materials composition at the various reaction stages was obtained by NMR spectroscopy.[18]
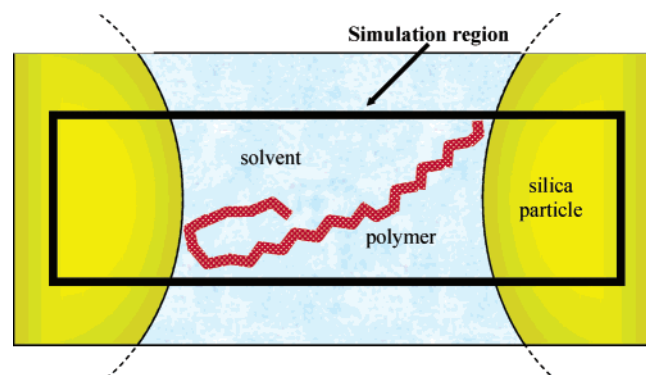
Polymer Interactions with Silica Particles

J. Phys. Chem. B, Vol. 107, No. 36, 2003 **9683**

Figure 2. Schematic representation of the simulated system.

Structural and dynamic developments of the model systems representing stages of the hydrolysis reaction were observed and interpreted in terms of fundamental intermolecular interactions and their effects on molecular mechanisms of the initial phase of the sol−gel process.

It was proposed that the formation stages of OIPH materials can be represented schematically, as shown in Figure 1. It was demonstrated[16,17] that, from the initially uniform solution (Figure 1a), organically modified inorganic precursors formed aggregates in water due to the hydrophobic effect (Figure 1b), with hydrolysis and elimination reactions forming silica particles (Figure 1c).

The typical alcohol elimination and −Si−O−Si− bond formation reactions[19] are shown below:

$$\equiv Si-OH + Si-OR \rightarrow \equiv Si-O-Si\equiv + ROH$$

$$\equiv Si-OH + Si-OH \rightarrow \equiv Si-O-Si\equiv + H_2O$$
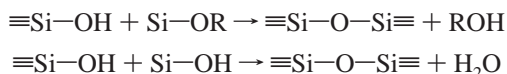
Although most of the eliminated alcohol molecules can be expected to dissolve and evaporate from solution, some residual ES fragments remain bonded to the silica surfaces in addition to the surface silanol (Si−OH) groups.[14]

It has also been shown[16,17] that the growth of the silica clusters at the stage shown in Figure 1b was limited by the polymer constituent, which attached itself to the clusters, thus preventing uncontrolled growth and precipitation of SiO_2 particles from the solution. During the final stages of the formation process, the silica particles are bonded together with PVA trapped between the particles while water evaporates (Figure 1d). For coatings applications this final OIPH product is formed when the OIPH solution is spread onto a substrate and dried to form a solid film.

The goal of the present work was to investigate the molecular interactions of PVA with the silica particles in solution which represents the formation stage of the OIPH material schematically shown in Figure 1c.

2. Molecular Models of OIPH Components

The model system considered here is schematically shown in Figure 2. The simulated region was represented in full atomistic detail, including chemical modifications of the silica surfaces, and explicit solvent (water) molecules, as described in the following sections. The effects of the silica surface residual modifiers, polymer solution concentration (polymer/water weight ratio), and distance between the silica particles on the polymer interaction with the particles have been investigated.

The molecular models developed in this work represent two SiO_2 surfaces separated by a layer of polymer aqueous solution.
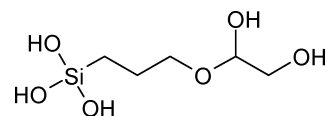

Figure 3. Hydrolyzed epoxysilane molecule.

By changing the distance between the surfaces, one can mimic two particles approaching one another while monitoring the changes adopted by the polymer. Furthermore, by changing the polymer/water volume ratio, the drying process can be simulated while also monitoring the polymer behavior between the particle surfaces. Clearly, the configuration space accessible to the polymer chain will be severely limited by the progressively reduced volume available between the surfaces and the polymer conformations will be strongly affected by the close presence of the surfaces and their chemical structure. Hence, the purpose of this work was to understand specific intermolecular interactions between the polymer chain and various surface residues within the imposed conditions.

2.1. Silica Surface Models. The original silica surface model used in the present study[21] has been previously employed for modeling alkyl modified silica surfaces.[8,22] In particular, a "hydrated" surface, containing the highest stoichiometrically possible number of surface silanols,[20] and a "dehydrated" surface, having the lowest OH surface density, have been developed. In place of silanols, other residues have also been employed, such as alkyl chains of various lengths. The modeled surfaces displayed typical structural features observed in experimental and/or other theoretical studies.[22]

As mentioned earlier, some ES groups may be attached to the surface of the silica particles considered in this work. To obtain this modified surface, all surface OH groups were replaced with the fully hydrolyzed epoxy silane residue depicted in Figure 3. The Si−C bond of this molecule was broken and the surface OH groups were replaced with the remaining residue. The total charge of the fragments was assigned to zero in order to retain overall neutrality of the system.

Intermediate structures, with different surface loadings were also constructed where only some of the OH groups were ES-modified. The residues were attached to the available sites on both sides of the silica "layer", keeping the loading densities as uniform as possible, to take advantage of the 3-D periodic boundary conditions (PBC). These systems included: fully modified (systems 1 and 4), intermediate (systems 2 and 5), and fully hydrolyzed (systems 3 and 6) systems, containing an OH/ES-residue surface density of 2.88, 0.75, and 0 per 100 $Å^2$, respectively (Table 1).

The created surface models placed in the unit cell were periodically replicated in three dimensions during the simulations. The dimensions of the unit cell were approximately 40×40 Å in the x- and y-directions, and the silica surface thickness, without considering the length of the surface modifiers, was approximately 17 Å (z-direction). A vacuum spacer was then incorporated in the z-direction to be filled by a polymer/water solution at a later stage. Given that the real particles in the studied OIPH formulation are up to 20 nm in diameter,[23,24] the thickness of the surface represents at least, or more than, 17% of the real particle radius. The unit cell surface area of 16 nm^2 represents approximately 2.5% of the surface area of the half-sphere of the 20 nm diameter. However, due to the periodic replication of the unit cell in the x- and y-directions, the larger surface area is actually mimicked. The adopted size of the SiO_2 surface was limited by the computer power available and the use of full atomistic details to simulate the systems, which were essential for the purpose of this study.

TABLE 1: Summary of the Simulated Systems

system no./type	polymer:water ratio	cell size in z-direction (Å)	description
1. modified	1:12.1	35	fully ES modified surface, with water and PVA
2. intermediate	1:14	35	partially hydrolyzed surface, with water and PVA
3. hydrolyzed	1:15.3	35	completely hydrolyzed surface, with water and PVA
4. modified	1:6.4	30	fully ES modified surface, with water and PVA; thinner water layer represents particles coming closer together
5. intermediate	1:7.5	30	partially hydrolyzed surface, with water and PVA; thinner water layer represents particles coming closer together
6. hydrolyzed	1:9.7	30	completely hydrolyzed surface, with water and PVA; thinner water layer represents particles coming closer together

By modeling the surfaces described above, different stages in the process can be examined and compared. In all cases, the periodicity of the systems in the z-direction was exploited to mimic the particles approaching each other by changing the cell size in the z-direction, i.e., the distance between the top and the bottom of the SiO_2 layer.

2.2. Polymer Model. The polymeric component, PVA, with a polymerization degree of 20, was constructed in line with previous studies on the earlier stages of the system formation[16,17] where relative scaling of the components was employed to retain the experimental weight ratios, to keep the system size computationally feasible.

The initial conformations of the PVA molecule were obtained using the Theodorou−Suter method,[25] which takes into account the realistic chain statistics. The polymer was placed at varying distances and initial orientations with respect to the surface to perform the simulations and collect statistics, therefore ensuring the observed trends are independent of the initial conformation and positioning of the polymer. One of the initial polymer configurations was used in the discussion section for comparison with the equilibrium configurations to illustrate trends in the systems.

2.3. Complete Model Systems. Once the silica surface models were constructed and the polymer was added to the system, the remaining available space in the simulation cell was filled with water molecules. A summary of the constructed model systems with varying surface chemistry and polymer/water weight ratios is presented in Table 1.

The initial cell height (z-direction of the unit cell) chosen to be 35 Å, is approximately twice the thickness of the silica surface. Due to the application of periodic boundary conditions, the surface is replicated in the z-direction, which allows the polymer to be under the influence of both "top" and "bottom" surfaces. Such an arrangement allows the effects of bringing these surfaces closer together to be examined by reducing the cell height.

As mentioned earlier, drying of the system can be simulated by systematically increasing the polymer/water weight or molar ratio in the model cell. The polymer interactions with the surfaces can then be examined as a function of the remaining water weight fraction as well as the distance between the surfaces. The initial polymer/water weight ratio in the 35 Å cell was 1:15.3 for the hydrolyzed surface, 1:14 for the intermediate surface and 1:13 for the ES-modified surface. These ratios are in line with the experimental ratio of 1:12.7 used in the original formulations.[10,18] To mimic the drying process, the ratio was increased by reducing the cell height, thus keeping the polymer component the same and decreasing the water fraction by reducing the volume available to be occupied by water. The polymer/water weight ratios at this reduced cell height of 30 Å were 1:9.7, 1:7.5, and 1:6.4 for the hydrolyzed, intermediate, and ES-modified surfaces, respectively.

2.4. Dry Systems. To complete the model, the final stages of the OIPH formation process were also simulated. As mentioned earlier, water is evaporated from the system during this final stage (Figure 1d); therefore water molecules added to the previously described molecular systems were removed to form three "dry" systems. To mimic the silica particles coming together, the cell height (z-direction) of each system was further decreased systematically, from 35 to 27 Å in 2 Å steps, generating a total of 15 model systems. Overlapping of surface residues with an image surface and/or residue prevented the cell height being reduced further than 27 Å. As for the wet systems, initial PVA chain configurations were selected at random from the generated equilibrium ensemble.

3. Simulation Procedures

Once the system had been prepared with all components, molecular dynamics (MD) simulations were performed. Each individual surface model underwent preliminary potential energy minimization after the construction process using the steepest descent method, followed by the conjugate gradient method.[26] In these simulations, as well as in all subsequent MD simulations, the silica surface was kept fixed to avoid altering the amorphous structure, with the exception of the surface residues which were allowed to relax.

The COMPASS force field,[27] which has been previously employed successfully to model polymer hydrogels and organic−inorganic systems[16,17] was chosen to model the potential energy of the systems. The atom-based summation method was used to evaluate the nonbonded van der Waals interactions with a cutoff distance of 15 Å.[26] The cell multipole method was used for evaluating Coulomb interactions.[25]

After the initial surface residue relaxation, each complete system was simulated by MD in the NVT ensemble at 298 K until equilibrium was reached, followed by the equilibrium data collection. The equilibrium was checked by monitoring temperature and potential energy fluctuations. The relatively small size of the polymer molecule resulted in equilibration within 2 ns.

The molecular modeling software from Accelrys, Inc. was used to create the models used in this study and to perform the calculations.

4. Results and Discussion

4.1. Time Dependent Behavior of the Aqueous Systems. A comparison between the initial and equilibrium polymer configurations between modeled surfaces was performed using the polymer distribution profiles before and during the equilibrium stage of the MD simulations, as shown in Figure 4.

In all systems (Figure 4), it appeared that the PVA does have an affinity toward a surface, independent of the initial orientation of the polymer. For all three (35 Å) systems (Figure 4a−c), the
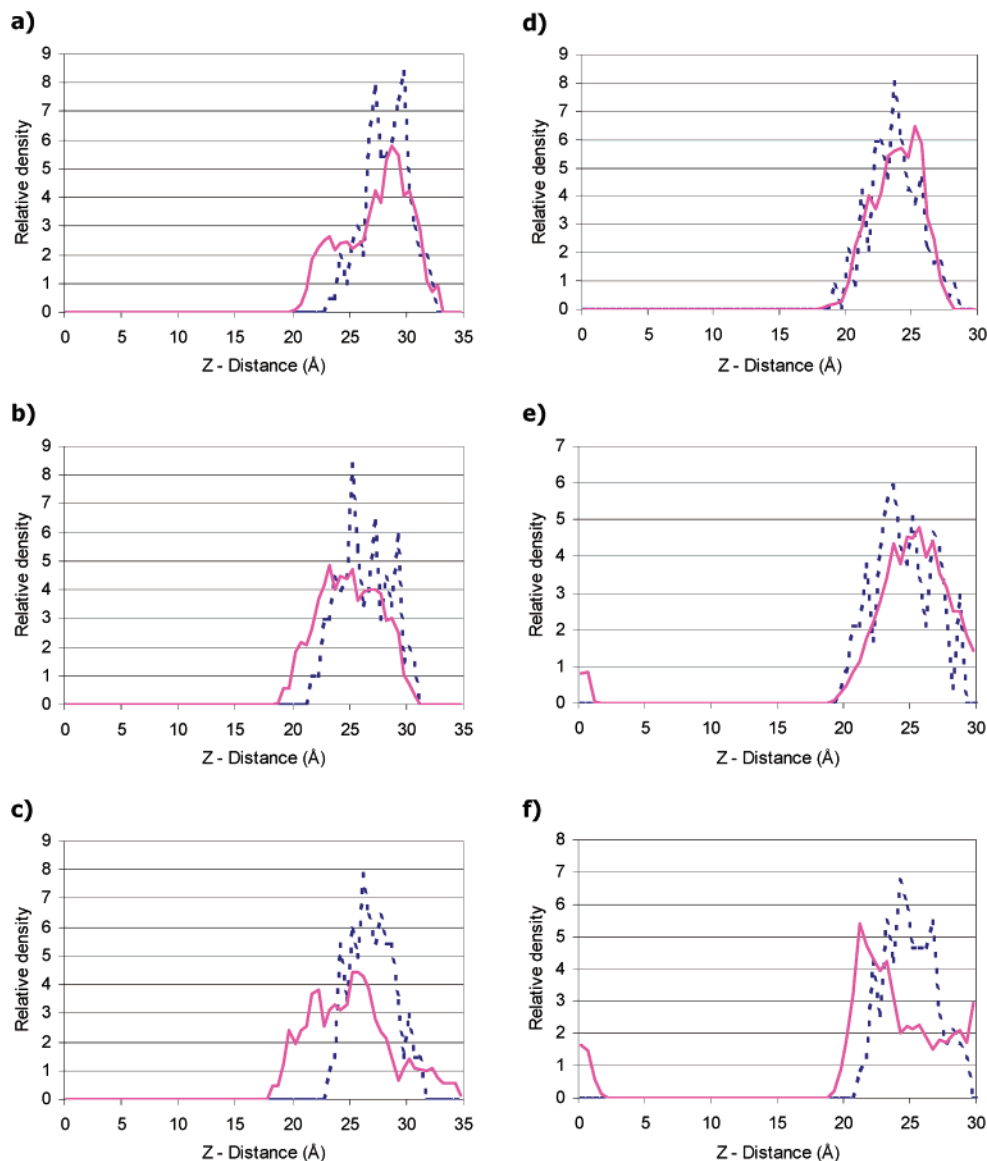
Polymer Interactions with Silica Particles

J. Phys. Chem. B, Vol. 107, No. 36, 2003 **9685**

Figure 4. Concentration profiles of PVA within the simulated systems with 35 Å cell height [(a) modified; (b) intermediate; (c) hydrolyzed] systems and 30 Å cell height [(d) modified; (e) intermediate; (f) hydrolyzed] systems. Key: (dotted) initial; (solid) equilibrium.

polymer appeared to have a higher affinity toward the top surface as shown by the shoulder observed between 20 and 25 Å (silica occupies the space between 2.5 and 19 Å). In the fully hydrolyzed system (Figure 4c), the nonzero polymer concentration near the top of the cell (30−35 Å) suggested that the polymer may be also attracted to the bottom surface, forming a bridge between the two particles.

In the 30 Å cell (Figure 4d−f), the changes in polymer distribution were less pronounced, with the exception of the fully hydrolyzed system (Figure 4f), where the bridging effect of the polymer was more evident. Although the polymer was better affiliated with the top surface, the density distribution around the cell boundaries (0 and 30 Å) suggested that a fragment of the polymer was attached to the opposite surface. The overall trend could therefore be described as the polymer preferring to affiliate with at least one silica particle in solution but may also serve as a bridge between particles by attaching to two of them at the same time (with a more significant affiliation with one of them).

4.2. Radial Distribution Functions in Aqueous Systems.
To elucidate specific interactions, and to analyze the role of

water in the system, radial distribution functions (RDFs) between specific chemical groups in the system were examined. OH groups within the polymer and silica surface were cross-examined with each other and with water molecules (H_2O). Two groups were considered to be hydrogen bonded if the O−H and O−O distances were around 1.8 and 2.8 Å, respectively. Interactions corresponding to a peak at 3.5 Å were interpreted as distorted H-bonds formed by interstitial water molecules observed in pure/bulk water.[28] The RDFs are presented in Figure 5.

It can be seen from Figure 5a that PVA was most attracted to the surface with intermediate loading as demonstrated by the higher peaks in $g(r)$ at atomic distances less than 5 Å. H-bond peaks were present for both modified and intermediate surfaces, however, they were smaller for the modified surface. This difference may arise from varying accessibility of the surface OH groups to the polymer, which is schematically illustrated in Figure 6.

For a high surface loading (fully modified), the fragments were closer to each other compared to the intermediate loading, forming a steric barrier that may have prevented the PVA from directly accessing the surface OH groups. Conversely, the
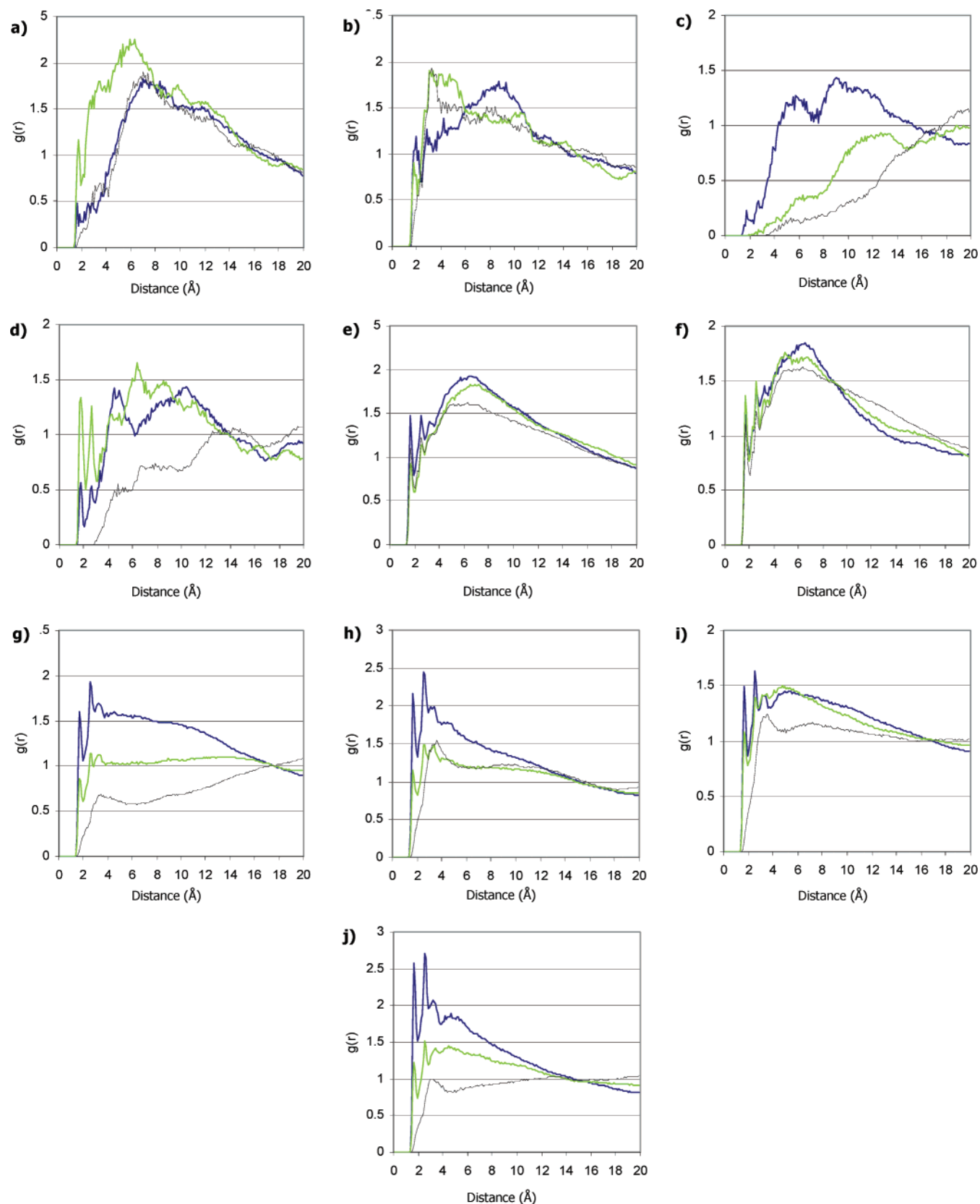
Figure 5. Radial distribution functions. Key: (blue line) modified system; (green line) intermediate system; (black line) hydrolyzed system. (a) PVA(OH) − top surface (OH&O), 35 Å cell; (b) PVA(OH) − top surface (OH&O), 30 Å cell; (c) PVA(OH) − bottom surface (OH&O), 35 Å cell; (d) PVA(OH) − bottom surface (OH&O), 30 Å cell; (e) PVA(OH) − H_2O, 35 Å cell; (f) PVA(OH) − H_2O, 30 Å cell; (g) H_2O − top surface (OH), 35 Å cell; (h) H_2O − top surface (OH), 30 Å cell; (i) H_2O − bottom surface (OH), 35 Å cell; (j) H_2O − bottom surface (OH), 30 Å cell.

silanols on the fully hydrolyzed surface do not possess the flexibility of the OH groups of the relatively long chain ES residue and thus are not as easily accessible to PVA. This may

also contribute to the distorted H-bonds observed in the fully hydrolyzed systems (at ∼3.5 Å). For an intermediate surface loading, the PVA was able to get closer to the surface because
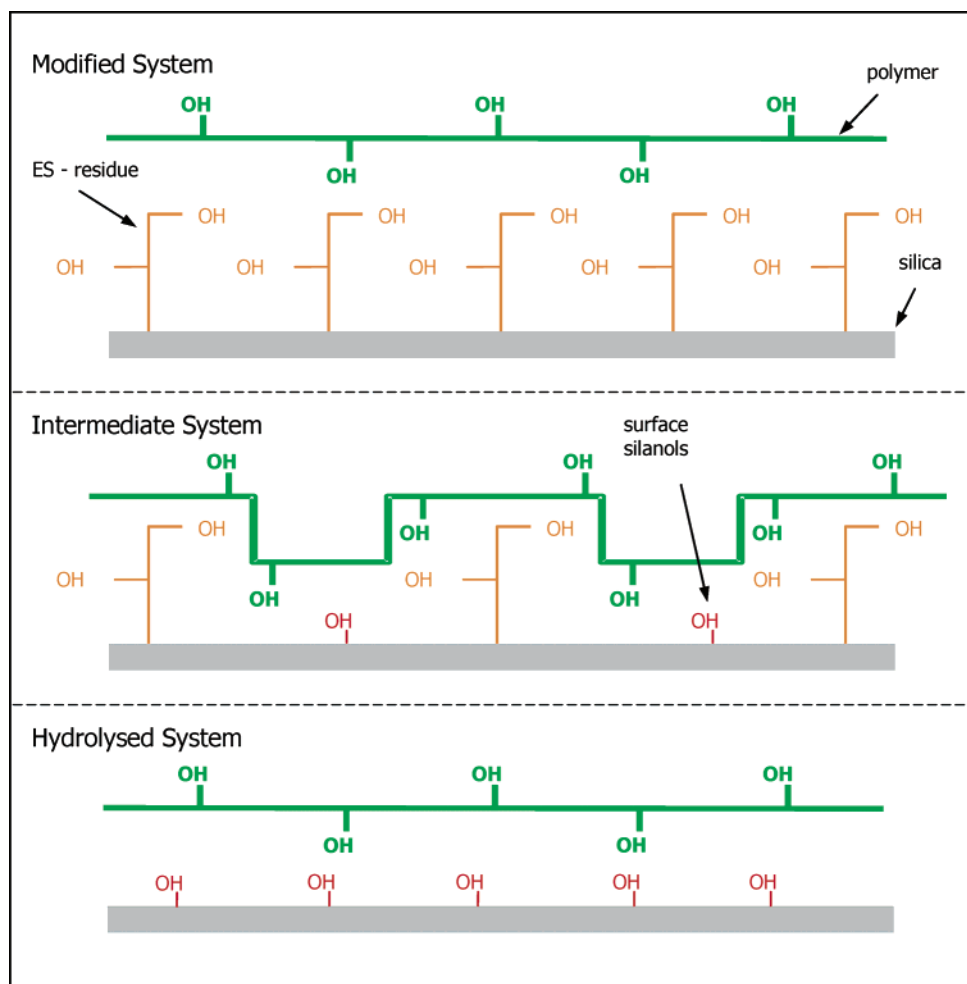
Polymer Interactions with Silica Particles

J. Phys. Chem. B, Vol. 107, No. 36, 2003 **9687**

Figure 6. 2-D schematic diagram of the proposed polymer and surface interactions in the three systems.

TABLE 2: Diffusion Constant, D ($\times 10^{-5}$ cm^2 s^{-1}), of Water Molecules in the Systems Simulated, Compared to Bulk Water

cell height (Å)	modified system	intermediate system	hydrolyzed system	bulk water[30] (298 K)
35	1.2	1.44	1.63	2.3
30	0.75	0.88	1.18	

the residues were located further from each other, allowing PVA to penetrate between them and form H-bonds with OH groups on the residues and the silanols. Therefore, in the intermediate system the effective contact area for the polymer–surface interactions was maximized compared to the other two surface loadings.

In Figure 5b, a shoulder was observed for the modified surface at short interatomic distances (with the exception of the H-bond peaks at 1.8 and 2.8 Å). This suggests that when the cell height was reduced, i.e., at low particle separation, the polymer had less interactions with the fully modified surface, probably due to the restricted movement within the limited space available. Dynamic properties shall be discussed in section 4.3.

From Figure 5a–d, it appeared that for all three surface loadings the polymer had a higher affinity toward the top surface, because for this surface the $g(r)$ value was higher at low particle separations than it was for the bottom surface. However, due to the equivalent character of the surfaces, this preference for one surface compared to the other most probably results from the initial positioning of the polymer. For the modified surface, typical O–H and O–O bonding peaks were observed at 1.8 and 2.8 Å, respectively, suggesting that the OH

groups on the polymer do form H-bonds with the hydroxyl groups on the ES residues. The increase in $g(r)$ values at small atomic distances may be due to sections of the polymer being attached to the surface as a result of polymer *partial* adsorption. The broad peaks at larger atomic distances (>4 Å) indicate that the bulk of the polymer lies further away from the surface. The polymer also appeared to be more attracted to the modified surface than the hydrolyzed surface (Figure 5c,d). This indicated that the PVA has a higher affinity toward the ES residues than the silanols in the fully hydrolyzed system. It can, therefore, be suggested that the residual surface ES residues are essential to achieve a better quality, more strongly bonded final OIPH product.

The fact that the polymer displayed a stronger tendency toward one of the surfaces suggests that macroscopically, under the influence of two silica particles in close proximity, PVA will ultimately favor one of the two, rather than stay at some equilibrium separation from both in the solution. This suggests that the interactions between the polymer and the silica surface are strong enough to cause the polymer adsorption on the inorganic particles.

In all systems, water molecules formed H-bonds with the OH groups of PVA (as illustrated by the sharp peaks at 1.8 and 2.8 Å in Figure 5e,f), which implies that water structures around the polymer.

Hydrogen bonds were also formed between the water and the OH groups of the modified surface systems (as seen by the peaks at 1.8 and 2.8 Å in Figure 5g–j). The increasing intensity of these peaks with greater ES loading of the surfaces suggests
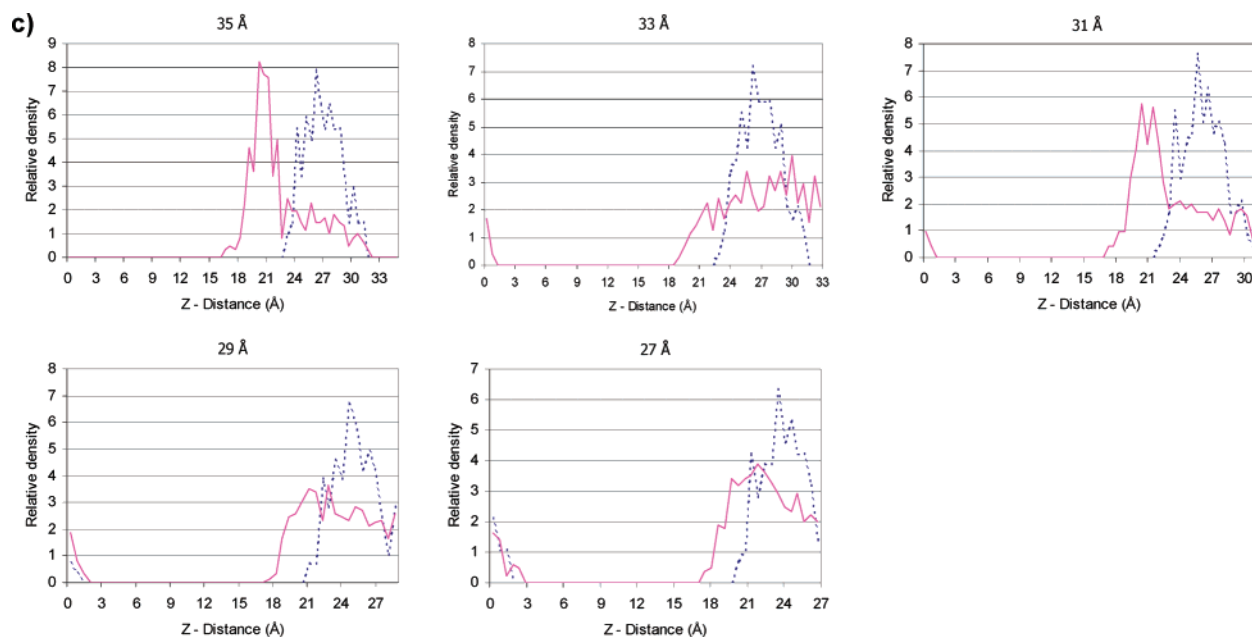
a)

b)
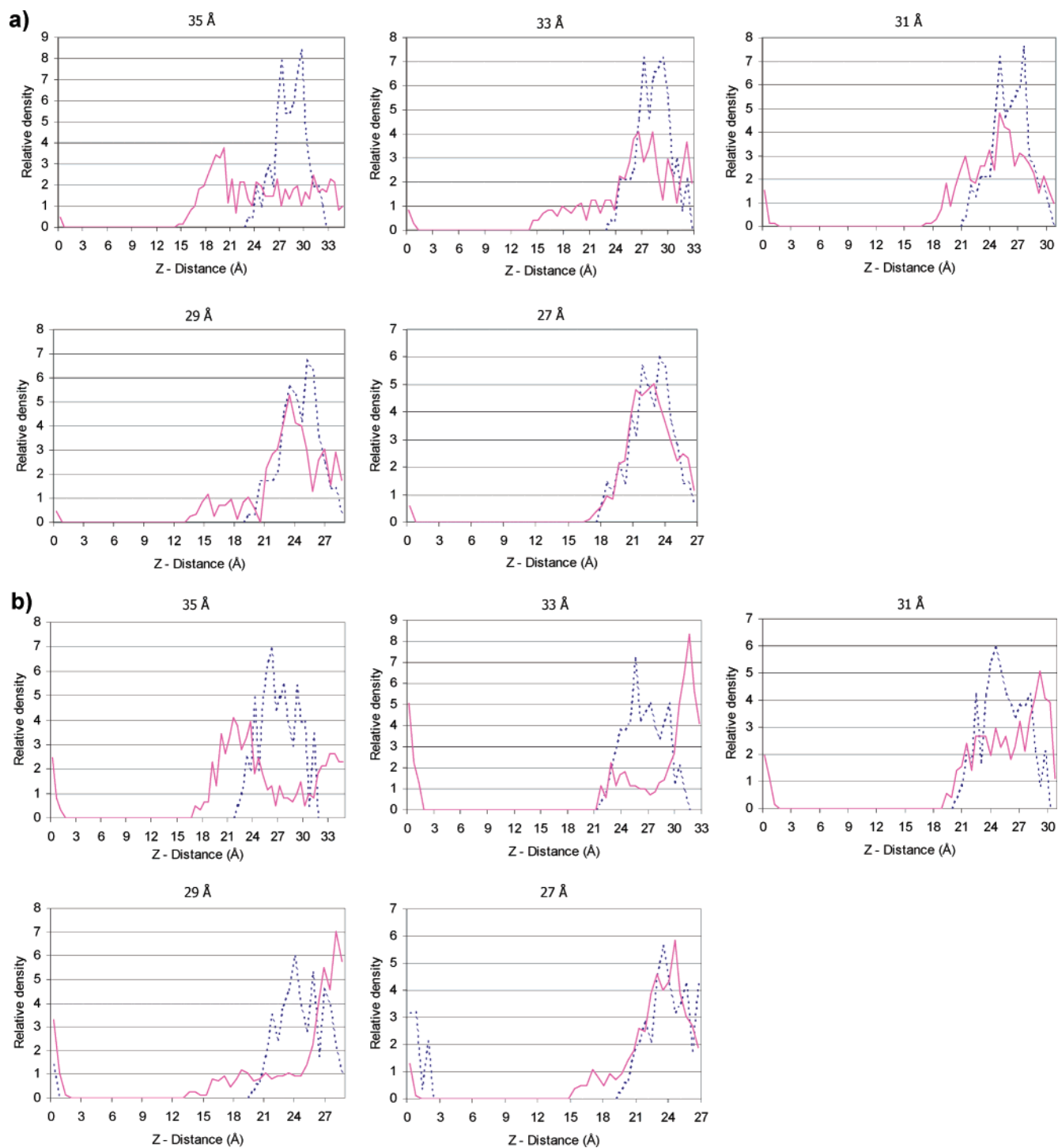
Figure 7. Concentration profiles of PVA in (a) the fully modified systems, (b) the intermediate systems, and (c) the hydrolyzed systems. Key: (dotted) initial; (solid) equilibrium.

that water interactions with the surfaces are enhanced by the presence of the residues. For the hydrolyzed system, the $g(r)$ value of distorted H-bonds from interstitial molecules[28] overshadows typical H-bond peaks, which indicates that water cannot access the silanols to form proper H-bonds and is instead structured around more accessible ES modifiers. Further information of the dynamic behavior of water may be elucidated through the analysis of the mean squared displacement of the molecules during the MD simulation.

4.3. Water Dynamics. Dynamic properties of water molecules were analyzed through their mean squared displacements (MSD), with diffusion coefficients (D) calculated from the Einstein relation[29] and displayed in Table 2. The experimental D value for bulk water at 298 K[30] is also shown for comparison.

The diffusion constant values in Table 2 show the decrease in mobility of water as the number of surface residues was increased, indicating that water molecules in the fully modified system diffuse slowest of all, probably because of the restricted movement from the presence of ES residues as suggested earlier. This may be explained by the increased number of H-bonds that water forms with the ES residues, as demonstrated by the RDFs. In addition, the diffusion of water molecules in all systems was significantly slowed by the reduction of the cell size, i.e., the particle separation distance, which mimicked the drying process. This effect can be explained by the fact that a more significant fraction of the remaining water molecules is hydrogen bonded to either the polymer or the surface, which results in the overall reduction of water mobility in the drying system.

4.4. Time Dependent Behavior of Dry Systems. Polymer distribution profiles showing the initial and equilibrium polymer configuration were determined for the fully modified, intermediate, and hydrolyzed dry systems for different cell heights and are displayed in Figure 7.

The polymer distributions show that the PVA displayed a higher affinity toward one surface, while maintaining a link with the opposite surface. This bridging effect was more pronounced compared to the previously analyzed "wet" systems, suggesting that drying of the system improved the networking of PVA with the silica. However, it could be observed that as the cell height

(and hence particle separation) was decreased, the movement of the polymer became more confined due to spatial limitations. At 27 Å, the movement of the polymer was completely restricted, as demonstrated by the similarity between the initial and equilibrium polymer distribution profiles (Figure 7, 27 Å).

4.5. Radial Distribution Functions in Dry Systems. For analysis of specific interactions, radial distribution functions between chemical pairs within the system were examined, as in the wet systems. RDFs of the polymer OH groups with the surface O and OH groups are displayed in Figure 8. The same H-bond peaks that were observed in the RDFs of the wet systems, at 1.8 and 2.8 Å, were also seen for the dry systems.

The results show that although there was no obvious correlation between particle separation and overall polymer–silica structuring (Figure 8a,c,d), independent analysis of the RDFs between the polymer and the top and bottom surfaces show that the polymer has preferential affinity toward one of the equivalent surfaces (Figure 8b,e,f).

Furthermore, this affinity appeared to diminish as the separation distance was reduced, until the polymer was evenly distributed between the two surfaces at 27 Å, where movement was almost completely restricted. In addition, peak intensities were clearly affected by the surface residue density. Structuring was more pronounced in the intermediate system with obvious hydrogen bond peaks at 1.8 and 2.8 Å (Figure 8c). Similar peaks were observed in the fully modified system (Figure 8a) with lower peak intensities, whereas the fully hydrolyzed system displayed no hydrogen bond induced polymer structuring (Figure 8e). This further supports the suggestion that the density of surface residues contributes toward polymer–silica networking (Figure 6).

5. Conclusions

Molecular models and procedures have been developed and tested to simulate interactions of PVA polymer with a range of modified silica surfaces in aqueous solution and in the dry state. Several informative trends have been observed for these systems that represent model stages of OIPH formation. The trends observed can be summarized as follows.
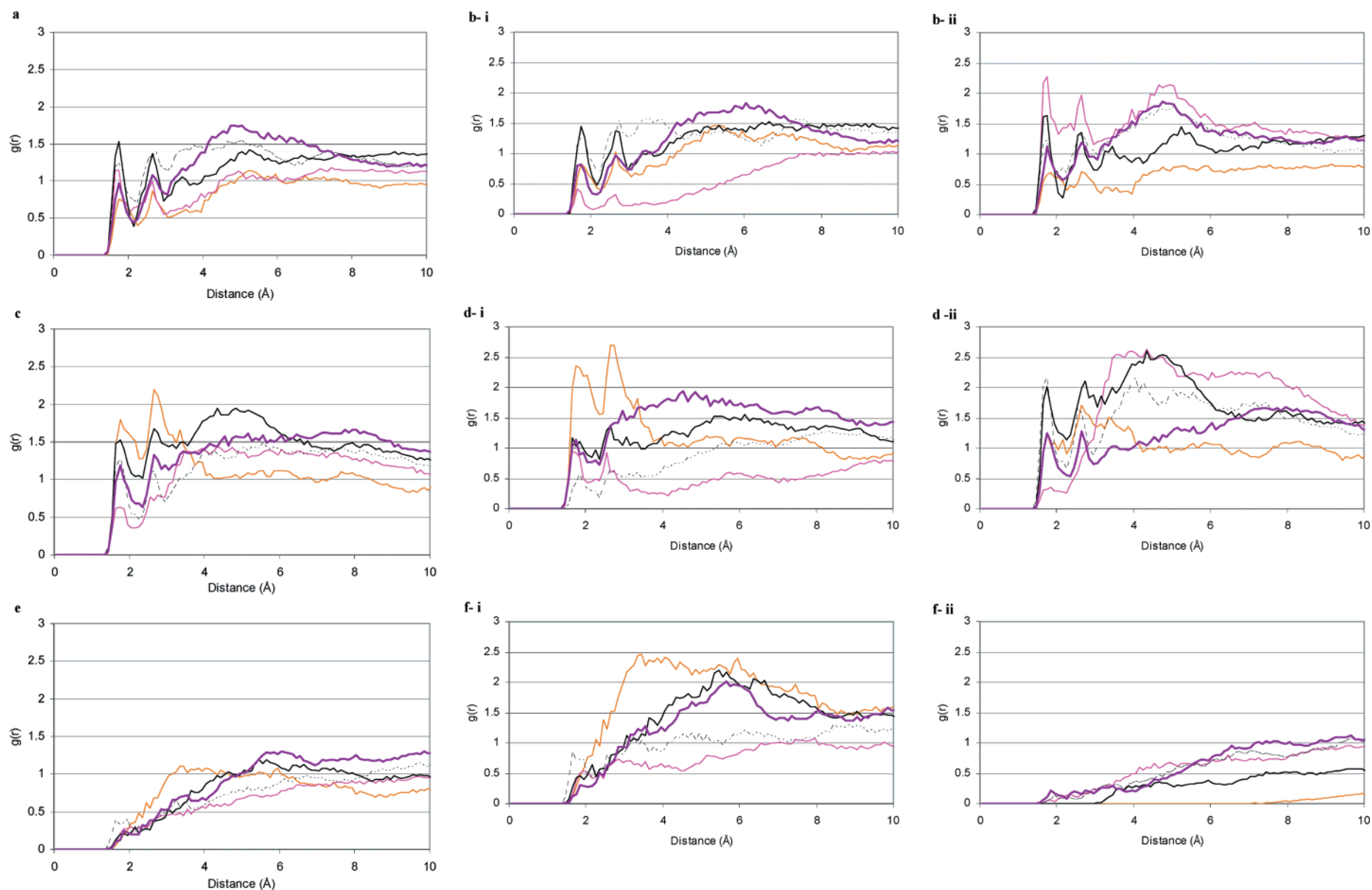
Figure 8. Radial distribution function of PVA OH groups and (a) both modified surfaces, (b-i) top surface, (b-ii) bottom surface, OH and O groups with decreasing cell height. Radial distribution function of PVA OH groups and (c) both intermediate surfaces, (d-i) top surface, (d-ii) bottom surface, OH and O groups with decreasing cell height. Radial distribuion function of PVA OH groups and (e) both hydrolyzed surfaces, (f-i) top surface, (f-ii) bottom surface, OH and O groups with decreasing cell height. Key: (orange) 35 Å cell height; (pink) 33 Å cell height; (black) 31 Å cell height; (dashed) 29 Å cell height; (purple) 27 Å cell height.

Polymer Interactions with Silica Particles

J. Phys. Chem. B, Vol. 107, No. 36, 2003 **9691**

As expected in the aqueous system, water was hydrogen bonded to the OH groups on the polymer and also to the OH groups on the silica surface and surface modifiers. In the ES-modified systems, water was more structured around the surface because of the higher concentration and easier accessibility of OH groups on the chain modifiers compared to the surface silanols. In both aqueous and dry systems, PVA was found to be more attracted to the modified surfaces due to the interactions with OH groups on the residues and surface silanols. The greater attraction toward the intermediate system may occur because the residues are located further from each other, thus increasing the interaction contact area with the PVA and allowing the polymer to interlock with them. It can be suggested that the attraction toward the ES-modified surface overall promotes PVA association with the silica particles. Therefore, the role of PVA is to provide a bridge between the particles that is facilitated by the presence of the residual ES groups on the particle surfaces.

The mobility of the system components decreased with increasing density of the surface modifiers as well as with drying, i.e., increasing polymer/water ratio, which was due to the increased portion of the hydrogen bonded water molecules in both cases.

References and Notes

(1) Schmidt, H. K.; Arpac, E.; Schirra, H.; Sepeur, S.; Jonschker, G. *Mater. Res. Soc. Symp. Proc.* **1998**, *519*, 297.

(2) Hoffmann, M.; Amberg-Schwab, S. *Mater. Res. Soc. Symp. Proc.* **1999**, *519*, 308.

(3) Klein, L. C.; Wert, J. V.; Beaudry, C. L. *Mater. Res. Soc. Symp. Proc.* **1999**, *576*, 337.

(4) Joel, J. E. M.; Man, M. W. C. *Mater. Res. Soc. Symp. Proc.* **1998**, *519*, 41.

(5) Laine, R. M.; Asuncion, M.; Baliat, S.; Filho, N. L. D.; Harcup, J.; Sutorik, A. C.; Viculis, L.; Yee, A. F.; Zhang, C.; Zhu, Q. Mater. *Res. Soc. Symp. Proc.* **1999**, *576*, 3.

(6) Katsoulis, D. E.; Chao, T. C.-S.; McQuiston, E. A.; Chen, C.; Kenney, M. E. *Mater. Res. Soc. Symp. Proc.* **1998**, *519*, 321.

(7) Kumudinie, C.; Mark, J. E. *Mater. Res. Soc. Symp. Proc.* **1999**, *576*, 331.

(8) Yarovsky, I.; Hearn, M. T. W.; Aguilar, M. I. *J. Phys. Chem. B* **1997**, *101*, 10962.

(9) Tamai, Y.; Tanaka, H. *Mol. Simul.* **1999**, *21*, 283.

(10) Tamai, Y.; Tanaka, H. *Macromolecules* **1996**, *29*, 6750.

(11) Luzar, A.; Chandler, D. *J. Chem. Phys.* **1993**, *98*, 8160.

(12) Nick, B.; Suter, U. W. *Comput. Theo. Polym. Sci.* **2001**, *11*, 49.

(13) Knopp, B.; Suter, U. W.; Gusev, A. A. *Macromolecules* **1997**, *30*, 6107.

(14) Muller-Plathe, F.; van Gusteren, W. F. *Polymer* **1997**, 38, 2259.

(15) Gestoso, P.; Brisson, J. *Comput. Theo. Polym. Sci.* **2001**, *11*, 263.

(16) Yarovsky, I.; Evans, E. *Mol. Simul.* **2002**, *28*, 993.

(17) Lay, H. C.; Yarovsky, I. *Mol. Simul.* **2003**, *29*, 231.

(18) Burger, I.; Evans, E. BHP Steel Research Laboratories, unpublished data, 1999.

(19) Landry, C. J. T.; Coltrain, B. K.; Brady, B. K. *Polymer* **1992**, *33*, 1486.

(20) Iler, R. K. *The Chemistry of Silica*; Wiley: New York, 1979.

(21) Garofalini, S. H. *J. Non-Cryst. Solids* **1990**, *120*, 1.

(22) Yarovsky, I.; Aguilar, M. I.; Hearn, M. T. W. *Anal. Chem.* **1995**, *67*, 2145.

(23) Evans, E. BHP Steel Research Laboratories, unpublished data, 2001.

(24) Yarovsky, I. Industrial Research Report, BHP Steel Pty. Ltd., RMIT University, 2000.

(25) Theodorou, D. N.; Suter, U. W. *Macromolecules* **1986**, *19*, 139.

(26) Discover, User Guide, Accelrys (Molecular Simulations Inc.) 1996.

(27) Sun, H. *Comput. Theo. Polym. Sci.* **1998**, *8*, 229.

(28) Jedlovszky, P.; Mezei, M.; Vallauri, R. *Chem. Phys. Lett.* **2000**, *318*, 155.

(29) Leach, A. R. *Molecular modelling − principles and applications*; Pearson Education Limited: England, 2001; p 381.

(30) Hertz, H. G. In *Water: a comprehensive treatise*; Franks, F., Ed.; Plenum Press: New York, 1973; Vol 3, p 301.